Article

Preparation of degradable superhydrophobic Mg/P/Z/F/H composite materials and their anticorrosion

Zhongxian Xi[a,b] Chengqing Yuan[a,b,*] , Xiuqin Bai[a,b] , Chun Wang[c] and Anne Neville[c]

[a]Reliability Engineering Institute, National Engineering Research Center for Water Transport Safety, MOST, Wuhan, 430063, China
[b]School of Energy and Power Engineering, Wuhan University of Technology, Wuhan, 430063, China
[c]Institute of Functional Surfaces, Department of Mechanical Engineering, University of Leeds, Leeds, United Kingdom
* Correspondence: author: E-mail: ycq@whut.edu.cn; Phone: 0086-027-86582035

Abstract: In this study, the degradable superhydrophobic Mg/P/Z/F/H (magnesium/poly(-caprolactone)/zinc oxide/1H,1H,2H,2H-perfluorodecyltriethoxysilane (PFDTES)/ heating process) composite materials were prepared through one-step method for enhancing the corrosion resistance of AZ91D magnesium alloys. Electrochemical measurements showed that Mg/P/Z/F/H materials significantly improved the corrosion resistance of magnesium alloys in 3.5 wt.% NaCl. The self-cleaning, adhesion and stability tests suggested that Mg/P/Z/F/H composite materials had well self-cleaning properties, good adhesion strength and stability in wet atmosphere.

Keywords: superhydrophobic surface; degradable; one-step method; Dip-coating; poly(ε-caprolactone) (PCL)

1. Introduction

With special solid-liquid adhesion, self-cleaning,[1-11] anti-icing,[4,6,7-11] anti-corrosion,[5,9,12,13] antibacterial and so on,[14-16] multifunctional super-antiwetting surfaces have recently attracted scientists' attentions to research superhydrophobic surfaces both in preparations and applications. And the present superhydrophobic materials researches focus on the undegradable polymer (epoxy resin, polyurethane, polytetrafluoroethylene , polyvinyl chloride, perfluoropolyalkylether. etc) and various metal alloys (Fe, Cu, Ni, Co) containing heavy metal ions.[17-22] With the wide application of metals and the undegradable polymer, the environment risks of various heavy metals (especially Pb, Cu, Cd, Cr, and Ni) and the plastic particle pollution is becoming seriously under different corrosive medium. Here the environmentally degradable materials (Magnesium, Polycaprolactone and ZnO) were used to prepare the multifunctional superhydrophobic constructional materials.

As one of the lightest metal, with a density two-thirds that of aluminium and one-quarter that of steel, magnesium alloys thus have the great potential to improve system performance and energy efficiency in aerospace, auto industry, shipbuilding, mobile electronics, and bioengineering applications because of the magnesium's excellent chemical, mechanical, biological and physical properties.[23-27] However, because of magnesium's poor corrosion resistance especially in the corrosive medium environment of Cl^-, the magnesium alloys' applications are limited.[27-31] Furthermore, containing rare heavy metal elements such as Cu, Ni and Pb, the magnesium alloys are environment friendly and used as the biodegradable metals.[25] As a typical aliphatic polyesters, poly (ε-caprolactone) (PCL) is nontoxic and ecofriendly to living organisms which is widely used in food packaging and pharmaceutical industry.[25,32-36] ZnO powders are used in electronic and optoelectronic devices, solar cells and pharmaceuti-

 doi:10.20944/preprints202108.0505.v1

cal engineering because of the high safety, low price, extraodinary opto-electronic property and lacking of polluting effects as a newer type of promising candidate.[35,37,38]

In this study, degradable and superhydrophobic M/P/Z/F/H composite materials were prepared through one-step method to solve the poor corrosion resistance of magnesium. As a widely applied and simple surface treatment technology, dip-coating can produce a relatively adherent, stable and uniform films on the surface of materials.[39-42] Using dip-coating method the rough Mg/P/Z/F/H structure was constructed, which can be prepared simply and protect the magnesium alloy better. Furthermore, 30minutes' heating process at 50°C can not only repair defects of the composite Mg/P/Z/F materials' surface but also rearrange the PCL and PFDTES molecules to make the composite surface from hydrophobic (96.5°) to superhydrophobic (159.0 °). The surface morphology, microstructure, adhesion strength, corrosion resistance and self-cleaning of the superhydrophobic Mg/P/Z/F/H composite materials were tested.

2. Experimental Section

2.1. Materials

The following chemicals were used without further modification: ethanol (Tianjin Damao Chemical Reagent Factory, China), dichloromethane (DCM) (Qingmei Chemical Reagent Factory, China), 1H,1H,2H,2H-perfluorodecyltriethoxysilane (PFDTES) (Guangzhou Hongcheng Biotechnology Science and Technology Co., LTD, China, 97%), PCL (Mw: 80,000, Solvay Specialty Polymers, China), ZnO powders (30nm, Beijing Shenghehaoyuan Tech. Co. Ltd., China). Die-cast AZ91D magnesium alloy (Dongguan Qingmei Metal Materials Co., Ltd., China) was used as a substrate material.

2.2. Sample preparation

In this work, die-casted Mg alloy (AZ91D) with a chemical composition (wt.) of 8.77% Al, 0.74% Zn, 0.18% Mn, 90.31% were cut into 25mm × 25mm × 5mm. Before used, the samples were polished by silicon carbide papers from 150 to 1000 mesh, then ultrasonically cleaned in acetone and rinsed by de-ionized water. Finally, the samples were dried at 60 °C.

2.3. Preparation of Mg/P/Z/F/H composite materials

By dip-coating method the Mg/P/Z/F composite materials were prepared as was shown in Scheme 1 with suitable concentrations of PCL solutions.

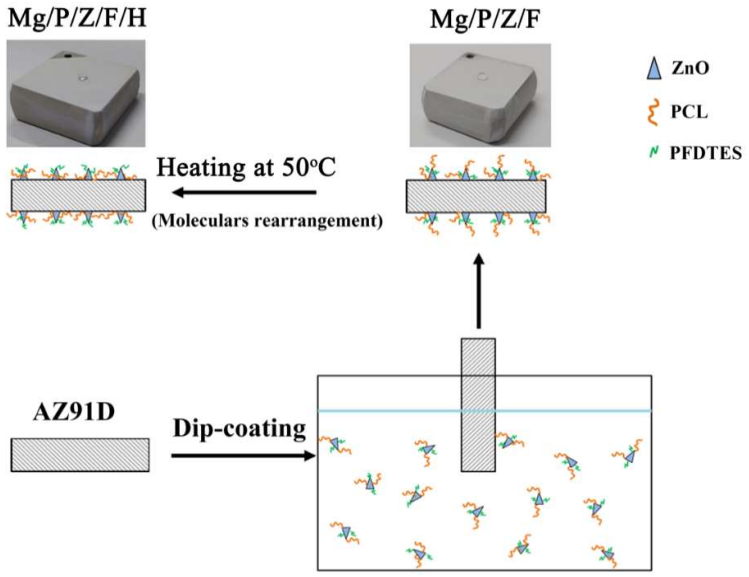

Scheme 1. Schematic illustration of fabricating superhydrophobic Mg/P/Z/F/H composite materials.

Under magnetic stirring for 5 h, PCL (5 wt.%) granules were dissolved in 60mL dichloromethane (DCM) solvent. Thenmixed the ZnO powders with PCL polymer solution (5 wt.%)and stirred continuously. Dropt 1.5mL PFDTES and stirred continuously for 10 h. The prepared samples were immersed into the mixed solutions for 30s and pulled out of the solution at a speed of 2 mm/s. Then the Mg/P/Z/F composite materials were prepared. After heating process of the Mg/P/Z/F materials at 50°C for 30min, the Mg/P/Z/F/H materials were gained. Table 1 showed the layers of five groups of the samples (Bare, Mg/P, Mg/P/Z, Mg/P/Z/F and Mg/P/Z/F/H).

Table 1. The coating of five groups of the samples.

Substrates	dip-coating concentrations	Treatment condition
Bare	None	None
Mg/P	5 wt.% PCL	None
Mg/P/Z	5 wt.% PCL; 5 wt.% ZnO	None
Mg/P/Z/F	5 wt.% PCL; wt.5% ZnO; 1.5mL PFDTES	None
Mg/P/Z/F/H	5 wt.% PCL; 5 wt.% ZnO; 1.5mL PFDTES	50°C, 30min

2.4. Surface characterization and property tests

Surface characterization experiments were performed via scanning electron microscopy and energy dispersive spectrometry at 10 kV (VEGA3, Tescan China Ltd., China). At ambient temperature the water contact angle were measured using an optical contact angle meter (Dataphysics OCA 15EC, Germany) with a 5μL water drop. Fourier transform infrared (FTIR, NEXUSFT-870, USA) spectra were recorded in the range of 400-4000cm^{-1}. Electrochemical tests were performed by electrochemical workstation (CorrTest CS350).

3. RESULTS AND DISCUSSION

3.1. Wetting behaviors

The wetting behaviors of four groups (Mg/P, Mg/P/Z, Mg/P/Z/F and Mg/P/Z/F/H) were tested in this study. The resulting surfaces showed different hydrophobicities of Mg/P, Mg/P/Z, Mg/P/Z/F and Mg/P/Z/F/H composite materials (Fig 1). In Fig 1a, we could see that the ecofriendly and degradable PCL coating was hydrophilic and the CA of Mg/P materials is 65.5±1.1° (Fig 1a). With the addition of ZnO powders, because of the ZnO could construct the micro-nano rough structure the CA of the Mg/P/Z was from 65.5±1.1° to 98.6±1.5° (Fig 1b). Then by mixing PFDTES at room temperature the Mg/P/Z/F materials were prepared. However, the CA of Mg/P/Z/F was similar as that of Mg/P/Z. In room temperature condition, mixing PFDTES did not change the wetting behaviors evidently and the CA of Mg/P/Z/F was 96.5±1.8° (Fig 1c). After 30 minutes' heating process at 50°C of the Mg/P/Z/F, we gained the Mg/P/Z/F/H and the CA of Mg/P/Z/F/H surface was 159.0±1.6° as was shown in Fig 1d.

 doi:10.20944/preprints202108.0505.v1

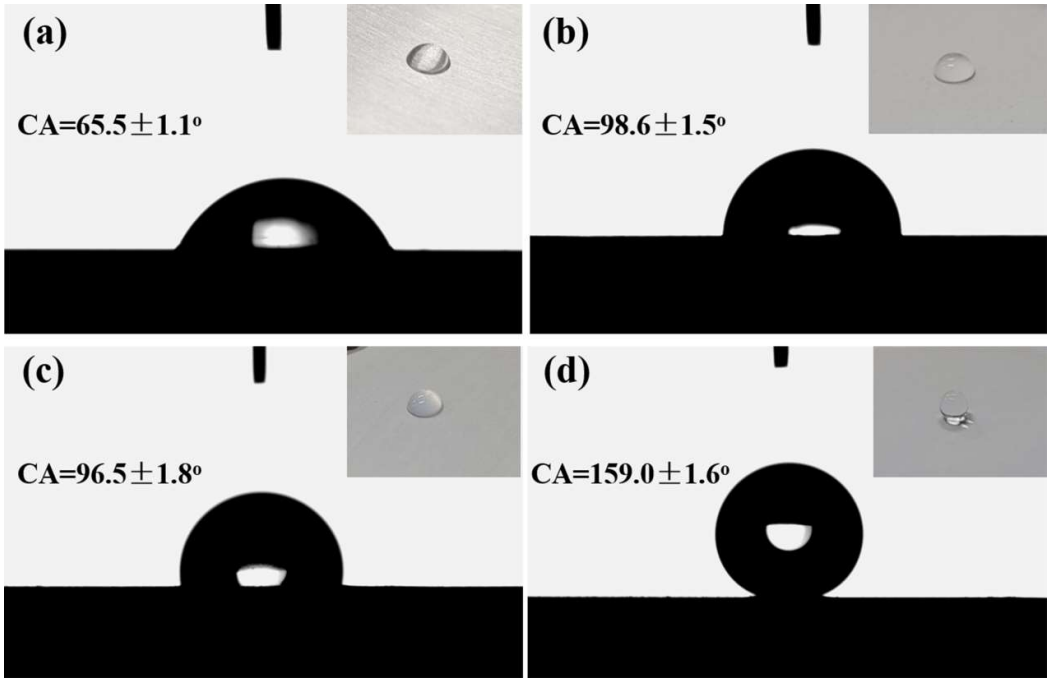

Figure 1. The images of the water droplet contact angles on Mg/P (a), Mg/P/Z (b), Mg/P/Z/F (c), Mg/P/Z/F/H (d) samples.

3.2. Surface characteristics

The SEM and EDS surface morphology of M/P/Z, M/P/Z/F and M/P/Z/F/H composite materials were shown in Fig 2. The Mg/P/Z exhibits a heterogeneous surface with micro-scaled roughness and high porosity (Fig 2a and 2d). In Fig 2b and 2e, the Mg/P/Z/F materials were prepared with low porosity and the ZnO particles were bonded evenly together by the PCL. However, we could observe that there were many gully defects on the surface of M/P/Z/F composite materials. After 30 minutes, heating process at 50°C the gully defects were repaired and the surface of the M/P/Z/F/H became superhydrophobic (Fig 2c and 2f). In the former study, after heating process the Mg/P/Z/F at 35°C and 45°C for 30minutes, the CA of the composite materials' surface did not change obviously and the CA was about 98°. In addition, the EDS of Mg/P/Z (Fig 2g), Mg/P/Z/F (Fig 2h) and Mg/P/Z/F/H (Fig 2i) illustrate that without heating process the contents of PFDTES was tested low on the surface of Mg/P/Z/F (Si: 0.28 wt.%; F: 2.14 wt.%). However, after heating process at 50°C the contents of PFDTES increased apparently on the surface of Mg/P/Z/F/H (Si: 0.34 wt.%; F: 4.26 wt.%).

 doi:10.20944/preprints202108.0505.v1

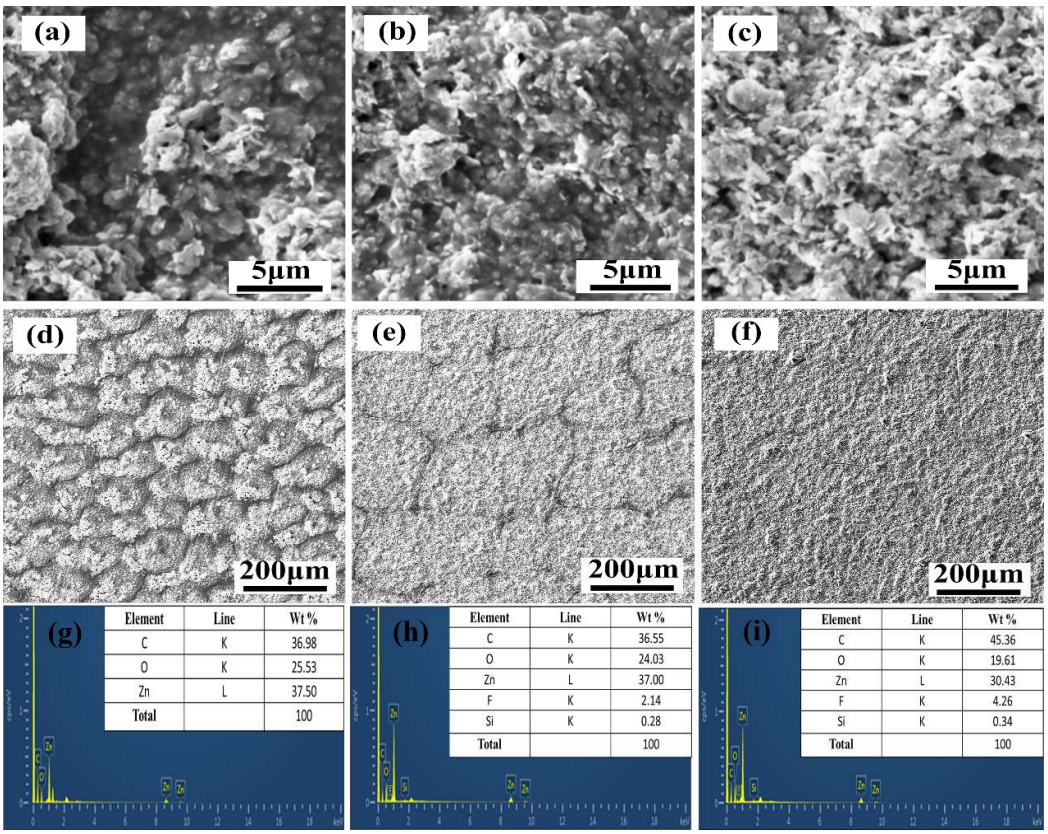

Figure 2. SEM micrographs of Mg/P/Z composite materials (a and d); Mg/P/Z/F composite materials (b and e); Mg/P/Z/F/H composite materials (c and f) and EDS of Mg/P/Z (g); Mg/P/Z/F (h); Mg/P/Z/F/H (i).

The compositions of Mg/P, Mg/P/Z, Mg/P/Z/F and Mg/P/Z/F/H were further analyzed via Fourier transform infrared spectroscopy (FTIR) as shown in Fig 3. Furthermore, at approximately 2956 and 2875 cm^{-1} vibrations generated by CH3 [υ (CH_3)] for the Mg/P, Mg/P/Z, Mg/P/Z/F and Mg/P/Z/F/H, vibrations generated by CH3 [υ (CH_3)] at approximately 2956 and 2875 cm^{-1}. At 1172 cm^{-1} for Mg/P/Z/F and Mg/P/Z/F/H, CF3 stretching vibrations [υ (CF_3)]appeared.[43,44] At 832 cm^{-1} for Zn-O stretching for Mg/P/Z/F/H could explain that after heating process the PCL transfer occurs on ZnO.[45] The FTIR tests were consistent with the EDS results and after heating process the ZnO powders were exposed.

 doi:10.20944/preprints202108.0505.v1

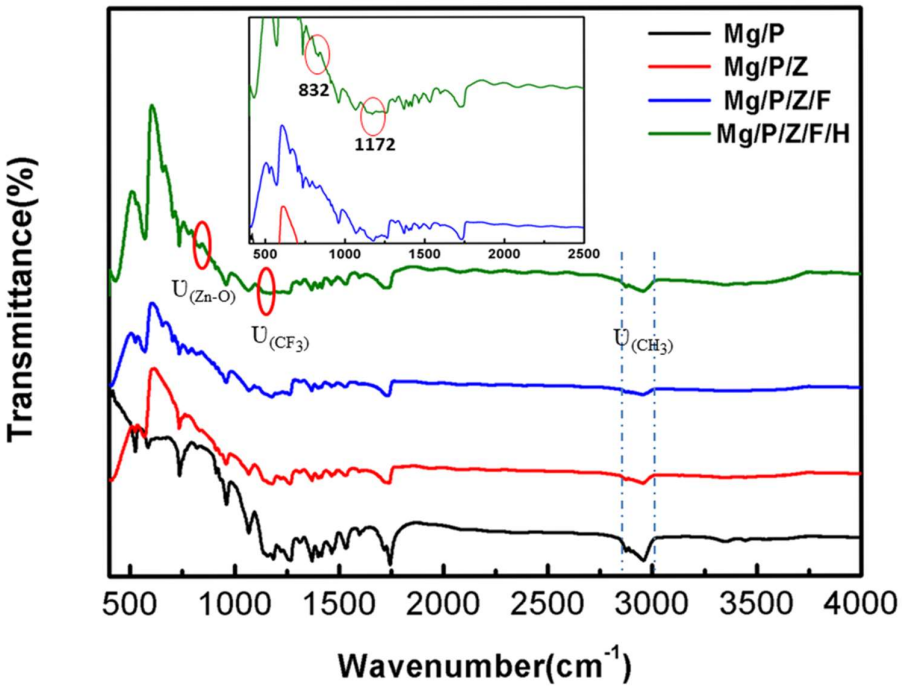

Figure 3. FTIR analysis curves of Mg/P, Mg/P/Z, Mg/P/Z/F and Mg/P/Z/F/H composite materials.

Here we propose the molecules rearrangement mechanism to explain the hydrophobic and superhydrophobic change process at softening temperature of PCL (50°C). The molecules rearrangement mechanism was as shown in Fig 4. At the softening temperature (50°C, about 9°C lower than the melting point of PCL (Mw: 80,000)) the PCL molecules could move more violently and freely. At the same time, the incarceration ability of PCL is weakened to the PFDTES. After 30minutes' heating process, the PFDTES and PCL molecules cause molecules rearrangement and the PFDTES molecules are exposed on the surface of the composite M/P/Z/F/H materials to form the superhydrophobic surface (Fig 4). Furthermore, frequent molecular motion could repair the gully defects of the surface of the M/P/Z/F/H materials (Fig 2c and f).

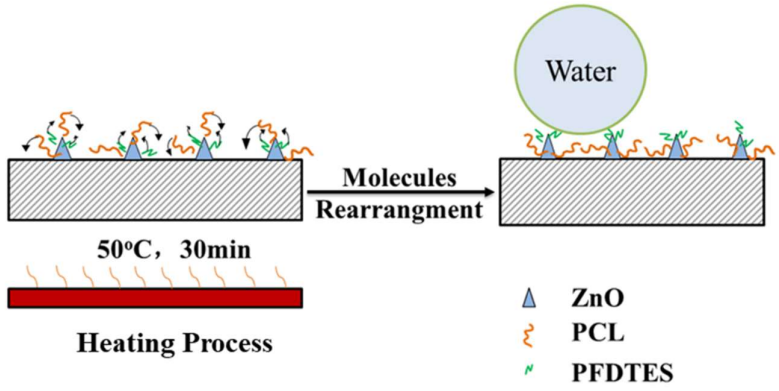

Figure 4. The process of the M/P/Z/F changing to M/P/Z/F/H at 50°C.

3.3. Electrochemical corrosion behavior

 doi:10.20944/preprints202108.0505.v1

With a three-electrode system in 300 mL 3.5 wt.% NaCl electrochemical impedance spectra (EIS) were carried out. Samples were exposed with a surface area of 1 cm^2. A saturated calomel and a platinum mesh electrode were used as the reference and the counter electrode, respectively. In Fig 5 the EIS plots of the five groups (Bare, Mg/P, Mg/P/Z, Mg/P/Z/F and Mg/P/Z/F/H) were reflected in 3.5 wt.% NaCl after a proper stabilization time (about 40min to 60min). In the Nyquist plane the impedance value of the working electrode is represented by the diameter of the capacitive loop.[25] As shown in Fig 5, Mg/P/Z/F/H samples showed the best anticorrosion performance The value of Rct for the Mg/P/Z/F/H samples (>1.5×10^7 Ωcm^2) is about 2×10^4 times larger than that of the Bare samples (750Ωcm^2). EIS results of Mg/P/Z/F/H samples indicated that after heating process the superhydrophobic samples Mg/P/Z/F/H samples could have desirable anti-corrosion performance.

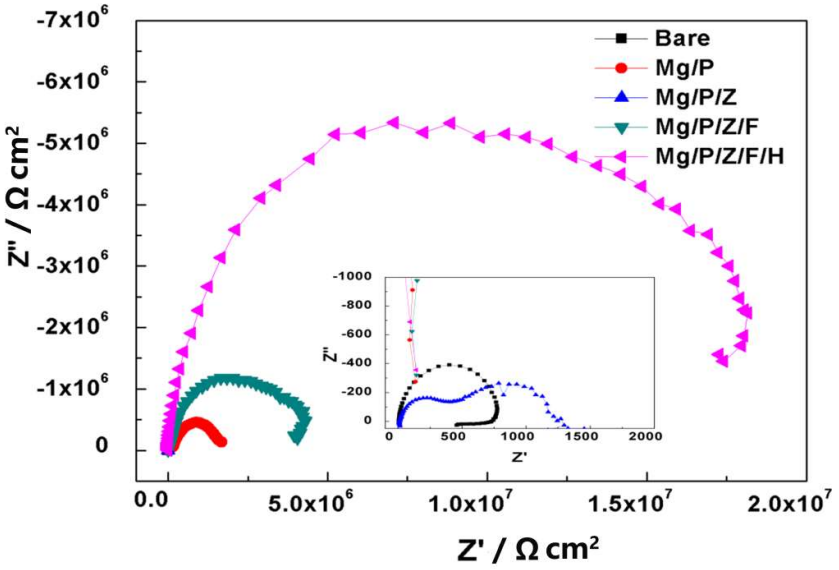

Figure 5. Electrochemical impedance spectroscopy (EIS) of samples in 3.5 wt.% NaCl.

Besides, corrosionpotential (E_{corr}), corrosioncurrentdensity (i_{corr}) and corrosionrate (CR) were calculated by using Tafel extrapolation methods (Fig 6 and Table 2). The polarization carves could be a typical indication of the materials' stability. The substrate corrosion current density of the composite materials decreased significantlywith the repair the gully defectsrepaired and molecular rearrangement after heating process. By the Cassie-Baxter state, the air trapped of the micro/nanostructured surface can improve the hydrophobicity and corrosion resistance of Mg/P/Z/F/H materials.[40,41] The Mg/P/Z/F/H materials had the best corrosion resistance and the corrosion rate of Mg/P/Z/F/H was 1.9152×10^{-3} mm/y. Here we found that with the addition of ZnO the corrosion resistance of Mg/P/Z sample decreased obviously because the ZnO powders destroyed the continuity of PCL layer (Fig 2d). And with the mixing of PFDTES the layer's discontinuity was modified (Fig 2e). Furthermore, the Mg/P/Z/F/H materials' main component parts are PCL, ZnO and magnesium alloys with the degradation and biocompatibility.[46-49]

 doi:10.20944/preprints202108.0505.v1

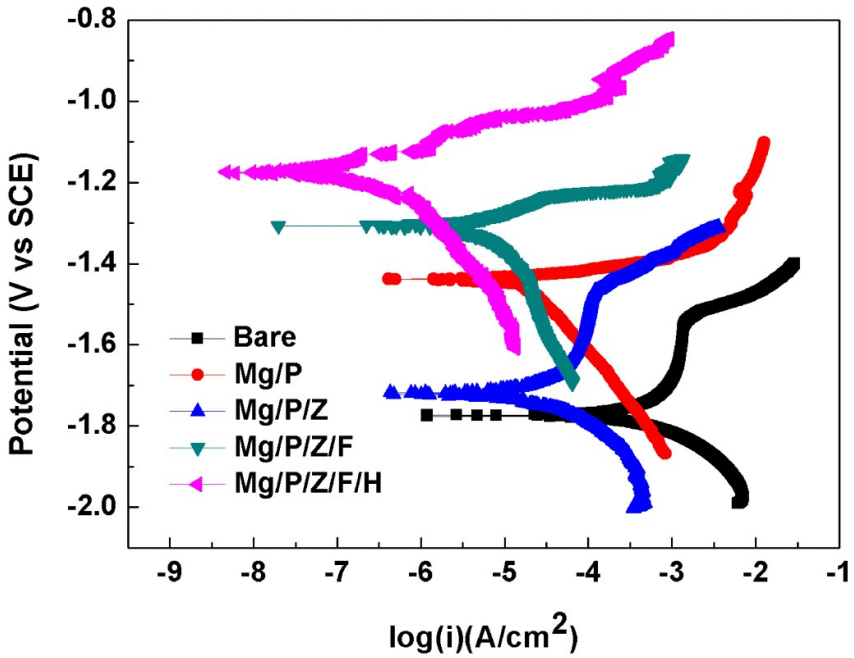

Figure 6. Polarization curves of the Bare, Mg/P, Mg/P/Z, Mg/P/Z/F and superhydrophobic Mg/P/Z/F/H.

Table 2. Electrochemical parameters of samples.

Substrates	I_{corr}(A/cm²)	E_{corr}(V)	Corrosion rate(mm/y)
Bare	1.0237×10^{-3}	-1.7694	22.0580
Mg/P	1.7464×10^{-5}	-1.6203	0.3763
Mg/P/Z	1.6043×10^{-5}	-1.7200	0.3457
Mg/P/Z/F	7.1288×10^{-6}	-1.3073	0.1536
Mg/P/Z/F/H	8.7914×10^{-8}	-1.1752	1.9152×10^{-3}

3.4. Interface model and anticorrosion mechanism

Water drops can have two states on a rough surface: Wenzel state and Cassie-Baxter state.[50,51] Here, with a low sliding angle the superhydrophobic surface could be explained by the Cassie-Baxter state. Micro/nanostructured surface can enhance the hydrophobic because the air trapped . And the heating process at 50°C could make the PFDTES molecules exposed on the surface of Mg/P/Z/F/H to form continuous air film as is shown in Fig 7. The continuous air film can sparate the substrate from the corrosive medium to improve the Mg/P/Z/F/H surface's hydrophobicity and corrosion resistance.

 doi:10.20944/preprints202108.0505.v1

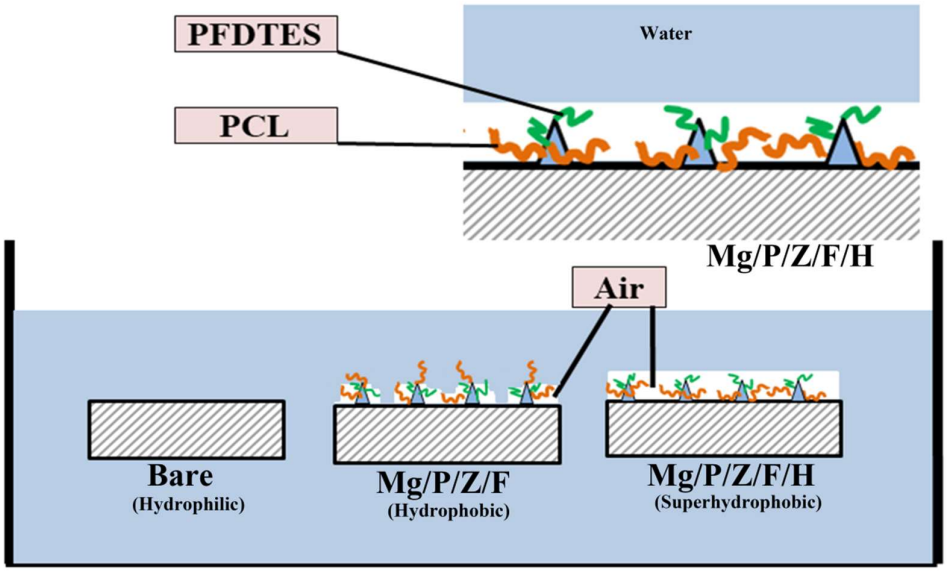

Figure 7. Anticorrosion mechanism of superhydrophobic surface in corrosive medium.

3.5. Stability and adhesion

For the practical application of materials, the stability is a highly important parameter. So the mechanical and superhydrophobic stability of materials' surfaces should be considered. In wet atmosphere at room temperature the stability of superhydrophobic was tested as is shown in Fig 8a. And the results illustrated that the superhydrophobic M/P/Z/F/H surface was stable and the CA of M/P/Z/F/H surface was over 155° after 168h at wet atmosphere (Fig 8b, the variation ranges of CA were between +1.8° and -1.6°).

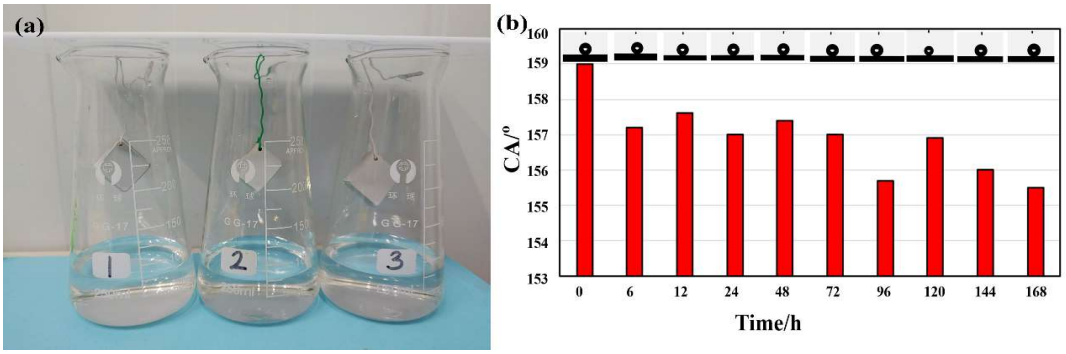

Figure 8. The wet atmosphere of the stability test (a) and the results of stability at wet atmosphere.

The mechanical adhesion stability of the surface was evaluated by using Scribe-Grid Test (ASTM D 3359-78).[25] Fig 9a and b shows the optical images of the superhydrophobic M/P/Z/F/H surface before (Fig 9a) and after (Fig 9b) the tape test. At the edges and within the square lattice there is no detachment or delamination of the film in Fig 9a and 9b. The adhesion of the resulting composite film corresponded to classification 4B according to ASTM D 3359-78. The results of mechanical adhesion stability clearly supported that the superhydrophobic M/P/Z/F/H sample was with strong adhesion to be applied in

 doi:10.20944/preprints202108.0505.v1

the engineering and industrial conditions.

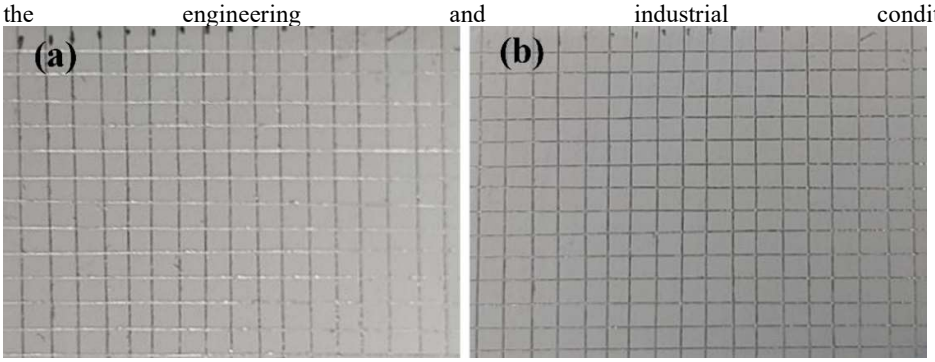

Figure 9. Images of the M/P/Z/F/H surface before (a) and after (b) the tape test.

3.6. Self-cleaning test

As an essential part of self-cleaning properties the ash adhesion resistance of the coating is tested by the chalk dust. Further, the self-cleaning ability of the superhydrophobic Mg/P/Z/F/H composite materials was shown in Fig 10. The Mg/P/Z/F/H samples were kept at an inclination of 10°. Each time 10μL water droplet was dropped from 20mm height to the red specified area. Simultaneously, the specified area was completely exposed after 10 water droplets and the water droplets took the chalk dust easily.

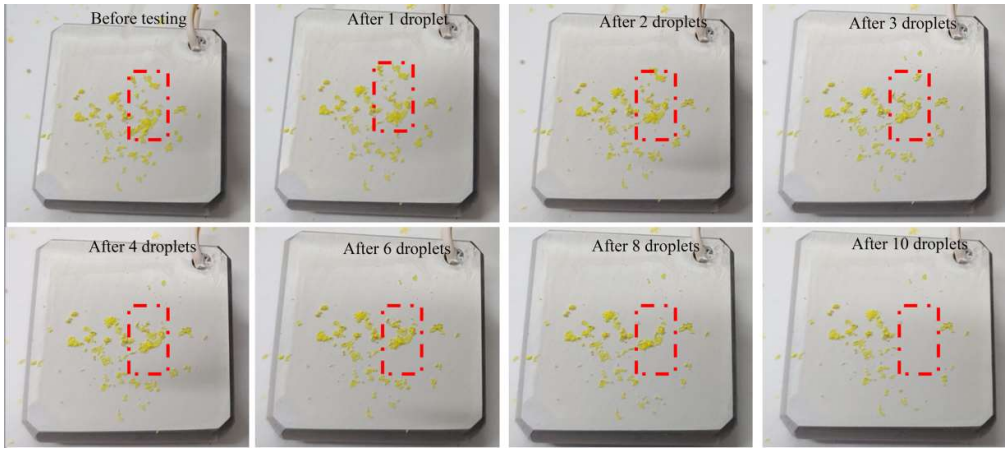

Figure 10. Self-cleaning properties of superhydrophobic the M/P/Z/F/H surface.

4. Conclusion

In this study, environmentally degradable superhydrophobic Mg/P/Z/F/H composite materials with less heavy metals were prepared successfully. And in 3.5 wt.% NaCl the electrochemical studies manifested that the Mg/P/Z/F/H had the outstanding corrosion resistance. About process of the superhydrophobic Mg/P/Z/F/H at 50°C for 30 minutes, we proposed the molecules rearrangement mechanism to explain the hydrophobic and superhydrophobic change process. What's more, the Mg/P/Z/F/H materials have well self-cleaning properties, good adhesion strength and stability in wet atmosphere and provide a feasible scheme in engineering technology and medical engineering application.

Author Contributions: All authors contributed equally.

Acknowledgments: The authors are grateful to the National Natural Science Foundation of China (Grant No. 52071246) for the support of this work.

References

1. J. Wei, G. Zhang, J. Dong, H.T. Wang, Y.L. Guo, X. Zhuo, C.G. Li, H. Liang, S.H. Gu, C.H. Li, X.Y. Dong, Y.F. Li, Scalable Spray-Coating of Stable Emulsion for Transparent Self-Cleaning Surface of Cellulose-Based Materials, ACS Sustainable Chemistry & Engineering, 6 (2018) 11335-11344.
2. L.J. Xiao, M. Deng, W.G. Zeng, B.X. Zhang, Z.S. Xu, C.F. Yi, G.F. Liao, Novel Robust Superhydrophobic Coating with Self-Cleaning Properties in Air and Oil Based on Rare Earth Metal Oxide, Industrial & Engineering Chemistry Research, 56 (2017) 12354-12361.
3. M. M. Tavakoli, K.H. Tsui, Q.P. Zhang, J. He, Y. Yao, D.D. Li, Z.Y. Fan, Highly Efficient Flexible Perovskite Solar Cells with Antireflection and Self-Cleaning Nanostructures, ACS nano, 9 (2015) 10287-10295.
4. B.Y. Chen, J.H. Qiu, E. Sakai, N. Kanazawa, R.L. Liang, Feng, H.X. Robust and Superhydrophobic Surface Modification by a "Paint + Adhesive" Method: Applications in Self-Cleaning after Oil Contamination and Oil-Water Separation, ACS Applied Materials & Interfaces, 8 (2016) 17659-17667.
5. T. Shi, X.X. Li, C.W. Zhang, H.X. Wang, Z.Y. He, X.G. Zhou, D.N. Yang, H,J. Yang, B.B. Zhang, K. Yang, One-step preparation of the superhydrophobic Al alloy surface with enhanced corrosion and wear resistance, Materials and Corrosion, (2020) 1-8.
6. J.L. Zhang, C.D. Gu, J.P. Tu, Robust Slippery Coating with Superior Corrosion Resistance and Anti-Icing Performance for AZ31B Mg Alloy Protection, ACS Applied Materials & Interfaces, 9 (2017) 11247-11257.
7. C.H. Qi, H. Chen, L.Y. Shen, X.L. Li, Q. Fu, Y.H. Zhang, Y.Y. Sun, Y.Q. Liu, Superhydrophobic Surface Based on Assembly of Nanoparticles for Application in Anti-Icing under Ultralow Temperature, ACS Applied Nano Materials, 3 (2020) 2047-2057.
8. Y.L. Zhang, L. Chen, Z.Z. Lin, L.J. Ding, X.F. Zhang, R.H. Dai, Q. Yan, X.D. Wang, Highly Sensitive Dissolved Oxygen Sensor with a Sustainable Antifouling, Antiabrasion, and Self-Cleaning Superhydrophobic Surface, ACS Omega, 4 (2019) 1715-1721.
9. R. Liu, Z.D. Chi, L. Cao, Z.K. Weng, L. Wang, L. Li, S. Saeed, Z.X. Lian, Z.B. Wang, Fabrication of biomimetic superhydrophobic and anti-icing Ti6Al4V alloy surfaces by direct laser interference lithography and hydrothermal treatment, Applied Surface Science, 534 (2020) 147576 (1-8).
10. J. Lin, C. Zheng, W.J. Ye, H.Q. Wang, D.Y. Feng, Q.Y. Li, B.W. Huan, A Facile Dip-Coating Approach to Prepare SiO_2/Fluoropolymer Coating for Superhydrophobic and Superoleophobic Fabrics with Self-Cleaning Property, Journal of Applied Poymer Science, (2015) 41458 (1-9).
11. T. Darmanin, E.T. Givenchy, S. Amigoni, F. Guittard, Superhydrophobic Surfaces by Electrochemical Processes, Advanced Materials, 25 (2013) 1378-1394.
12. D.M. Zang, R.W. Zhu, W. Zhang, X.Q. Yu, L. Lin, X.L. Guo, M.J. Liu, L. Jiang, Corrosion Resistance: Corrosion-Resistant Superhydrophobic Coatings on Mg Alloy Surfaces Inspired by Lotus Seedpod, Advanced Functional Materials, 27 (2017) 1605446 (1-7).
13. Q. Liu, D.X. Chen, Z.X. Kang, One-step electrodeposition process to fabricate corrosion-resistant superhydrophobic surface on magnesium alloy, ACS Applied Materials & Interfaces, 7 (2015) 1859-1867.
14. T. Suryaprabha,; M.G. Sethuraman, Fabrication of copper-based superhydrophobic self-cleaning antibacterial coating over cotton fabric, Cellulose, 24 (2017) 395-407.
15. C.H. Han, B.G. Min, Superhydrophobic and Antibacterial Properties of Cotton Fabrics Coated with Copper Nanoparticles through Sonochemical Process, Fibers and Polymers, 21 (2020) 785-791.
16. N. Ghasemi, J. Seyfi, Asadollahzadeh, M.J. Imparting superhydrophobic and antibacterial properties onto the cotton fabrics: synergistic effect of zinc oxide nanoparticles and octadecanethiol, Cellulose, 25 (2018) 4211-4222.
17. H.M. Zhou, R.R. Chen, Q. Liu, J.Y. Liu, J. Yu, C. Wang, M.L. Zhang, P.L. Liu, J. Wang, Fabrication of ZnO/epoxy resin superhydrophobic coating on AZ31magnesium alloy, Chemical Engineering Journal, 368 (2019) 261-272.
18. C. Bonneaud, J. Howell, R. Bongiovanni, C. Joly-Duhamel, C.M. Friesen, Diversity of Synthetic Approaches to Functionalized Perfluoropolyalkylether Polymers, Macromolecules, 54 (2021) 521-550.
19. Y.Z. Tang, H.L. Huang, X.Y. Guo, C.L. Zhong, Superhydrophobic Ether-Based Porous Organic Polymer-Coated Polyurethane Sponge for Highly Efficient Oil-Water Separation, Industrial & Engineering Chemistry Research, 59 (2020) 13228-13238.
20. J. Tam, Z.H. Jiao, J.C.F. Lau, U. Erb, Wear stability of superhydrophobic nano Ni-PTFE electrodeposits, Wear, 15 (2017) 374-375 (1-4).
21. J.K. Liu, Y.B. Ouyang, R. Qiu, B.J. Ma, Y. Zhang, S.G. Hu, Compositing fluid infused in superhydrophobic $Cu(OH)_2$ nanoneedle matrix to inhibit abiotic and microbiologically induced corrosion of Cu in seawater environment, Progress in Organic Coatings, 142 (2020) 105542 (1-10).
22. S.N.K. Abad, N.N. Ilkhechi, M. Adel, M. Mozammel, Hierarchical architecture of a superhydrophobic Cd-Si co-doped TiO_2 thin film, Applied Surface Science, 533 (2020) 1474952.
23. T.M. Pollock, Materials science. Weight loss with magnesium alloys, Science, 328 (2010) 986-987.
24. D. Tie, H.N. Liu, R.G. Guan, P. Holt-Torres, Y.K. Liu, Y. Wang, N. Hort, In vivo assessment of biodegradable magnesium alloy ureteral stents in a pig model, Acta Biomaterialia, 116 (2020) 415-425.
25. Z.X. Xi, C. Tan, L. Xu, N. Yang, Q. Li, Preparation of novel functional Mg/O/PCL/ZnO composite biomaterials and their corrosion resistance, Applied Surface Science, 351 (2015) 410-415.
26. F. Sterl, N. Strohfeldt, R. Walter, R. Griessen, A. Tittl, H. Giessen, Magnesium as Novel Material for Active Plasmonics in the Visible Wavelength Range, Nano Letters, 15 (2015) 7949-7955.

27. H.S. Su, Y. Liu, X. Gao, Y.F. Qian, W.J. Li, T.G. Ren, L. Wang, J.L. Zhang, Corrosion inhibition of magnesium alloy in NaCl solution by ionic liquid: Synthesis, electrochemical and theoretical studies, Journal of Alloys and Compounds, 791 (2019) 681-689.
28. G.L. Song, Recent Progress in Corrosion and Protection of Magnesium Alloys, Advanced Engineering Materials, 7 (2005) 563-566.
29. R.X. Qiu, C. Li, W. Tong, D.S. Xiong, Z.X. Li, Z.L. Wu, High-speed wire electrical discharge machining to create superhydrophobic surfaces for magnesium alloys with high corrosion and wear resistance, Materials and Corrosion, 71 (2020) 1711-1720.
30. Y.Y. Yang, J.C. Zhou, Q. Chen, R. Detsch, X.F. Cui, G. Jin, S. Virtanen, A.R. Boccaccini, In Vitro Osteocompatibility and Enhanced Biocorrosion Resistance of Diammonium Hydrogen Phosphate-Pretreated/Poly(ether imide) Coatings on Magnesium for Orthopedic Application, ACS Applied Materials & Interfaces, 11 (2019) 29667-29680.
31. D.H. Yu, H. Qiu, X.H. Mou, Z.L. Dou, N.L. Zhou, Q.R. Guo, N. Lyu, L. Lu, Z.L. Yang, N. Huang, One-Pot but Two-Step Vapor-Based Amine- and Fluorine-Bearing Dual-Layer Coating for Improving Anticorrosion and Biocompatibility of Magnesium Alloy, ACS Biomaterials Science & Engineering, 5 (2019) 4331-4340.
32. F. Wu, C.S. Liu, B. O'Neilla, J. Wei, Y. Ngothai, Fabrication and properties of porous scaffold of magnesium phosphate/polycaprolactone biocomposite for bone tissue engineering. Applied Surface Science. 258 (2012) 7589-7595.
33. L.J. Hou, X. Zhang, P.E. Mikael, L. Lin, W.J. Dong, Y.Y. Zheng, T.J. Simmons, F.M. Zhang, R.J. Linhardt, Biodegradable and Bioactive PCL-PGS Core-Shell Fibers for Tissue Engineering, ACS Omega, 2 (2017) 6321-6328.
34. Y.C.E. Li, J.H. Wang, Y.H. Wang, H.J. Shao, L.C. Young, T.H. Young, PCL-Blended Chitosan Substrates for Patterning the Heterotypic Cell Distribution in an Epithelial and Mesenchymal Coculture System, ACS Biomaterials Science & Engineering, 6 (2020) 4225-4235.
35. W. Yuan, C.Y. Li, C. Zhao, C.G. Sui, W.T. Yang, F.J. Xu, J. Ma, Facilitation of Gene Transfection and Cell Adhesion by Gelatin-Functionalized PCL Film Surfaces, Advanced Functional Materials, 22 (2012) 1835-1842.
36. A. Behl, V.S. Parmar, S. Malhotra, A.K. Chhillar, Biodegradable diblock copolymeric PEG-PCL nanoparticles: Synthesis, characterization and applications as anticancer drug delivery agents, Polymer,207 (2020) 122901 (1-11).
37. S.N. Katea, S˘. Hajduk, Z.C. Orel, G. Westin, Low Cost, Fast Solution Synthesis of 3D Framework ZnO Nanosponges, Inorgnic Chemistry, 56 (2017) 15150-15158.
38. R. Peter, K. Salamon, A. Omerzu, J. Grenzer, I.J. Badovinac, I. Saric, M. Petravic, Role of Hydrogen-Related Defects in Photocatalytic Activity of ZnO Films Grown by Atomic Layer Deposition, The Journal of Physical Chemistry C, 124 (2020) 8861-8868.
39. A.K. Riau, D. Mondal, M. Setiawan, A. Palaniappan, G. H. F. Yam, B. Liedberg, S.S. Venkatraman, J.S. Mehta, Functionalization of the Polymeric Surface with Bioceramic Nanoparticles via a Novel, Nonthermal Dip Coating Method, ACS Applied Materials & Interfaces, 8 (2016) 35565-35577.
40. J.J. Fu, X.B. Li, L.X. Wang, X.H. Lv, Z.S. Lu, F. Wang, Q.Y. Xia, L. Yu, C.M. Li, One-Step Dip-Coating-Fabricated Core-Shell Silk Fibroin Rice Paper Fibrous Scaffolds for 3D Tumor Spheroid Formation, ACS Applied Bio Materials, 3 (2020) 7462-7471.
41. E. Bindini, G. Naudin, M. Faustini, D. Grosso, C. Boissière, Critical Role of the Atmosphere in Dip-Coating Process, he Journal of Physical Chemistry C, 121 (2017) 14572-14580.
42. F. Mirri, A.W.K. Ma, T.T. Hsu, N. Behabtu, S.L. Eichmann, C.C. Young, D.E. Tsentalovich, M. Pasquali, High-Performance Carbon Nanotube Transparent Conductive Films by Scalable Dip Coating, ACS Nano, 6 (2012) 9737-9744.
43. Y.H. Xie, X.F. Zhou, H.Y. Mi, J.H. Ma, J.Y. Yang, J. Cheng, High efficiency ZnO-based dye-sensitized solar cells with a 1H,1H,2H,2H-perfluorodecyltriethoxysilane chain barrier for cutting on interfacial recombination, Applied Surface Science, 434 (2018) 1144-1152.
44. Martins,P.; Lopes, A.C.; Lanceros-Mendez, S. Electroactive phases of poly (vinylidene fluoride): determination, processing and applications, Progress in Polymer Science, 39 (2014) 683-706..
45. L. Loh, J. Briscoe, S. Dunn, Chemical Protection of ZnO Nanorods at Ultralow pH To Form a Hierarchical $BiFeO_3$/ZnO Core-Shell Structure., ACS Applied Materials & Interfaces, 7 (2015) 152-157.
46. B. Felice, M. A. Sánchez, M. C. Socci, L. D. Sappia, M. I. Gómez, M. K. Cruz, C. J. Felice, M. Martí, M. I. Pividori, G. Simonelli, A. P. Rodríguez, Controlled degradability of PCL-ZnO nanofibrous scaffolds for bone tissue engineering and their antibacterial activity, Materials Science & Engineering C, 93 (2018) 724-738.
47. S. Mallakpour, M. Lormahdiabadi, Polycaprolactone/ZnO-folic acid nanocomposite films: Fabrication, characterization, in-vitro bioactivity, and antibacterial assessment, Materials Chemistry and Physics, 263 (2021) 124378.
48. J. Kim, H. M. Mousa, C. H. Park, C. S. Kim, Enhanced corrosion resistance and biocompatibility of AZ31 Mg alloy using PCL/ZnO NPs via electrospinning, Applied Surface Science, 396 (2017) 249-258.
49. M. Zhao, Y.K. Dai, X.B. Li, Y. Li, Y. Zhang, H.R. Wu, Z.H. Wen, C.S. Dai, Evaluation of long-term biocompatibility and osteogenic differentiation ofgraphene nanosheet doped calcium phosphate-chitosan AZ91D composites, Materials Science & Engineering C, 90 (2018) 365-378.
50. Z.X. She, Q. Li, Z.W. Wang, L.Q. Li, F.N. Chen, J.C. Zhou, Novel Method for Controllable Fabrication of a Superhydrophobic CuO Surface on AZ91D Magnesium Alloy, ACS Applied Materials & Interfaces, 4 (2012) 4348-4356.
51. A. B. D. Cassie, S. Baxter, Wettability of porous surfaces, Trans. Farad. Soc, 40 (1944) 546-550.